arXiv:1512.04503v3 [astro-ph.HE] 3 Jun 2016

# How Soft Gamma Repeaters Might Make Fast Radio Bursts

J. I. Katz

*Department of Physics and McDonnell Center for the Space Sciences*

*Washington University, St. Louis, Mo. 63130 USA*

katz@wuphys.wustl.edu

## ABSTRACT

There are several phenomenological similarities between Soft Gamma Repeaters and Fast Radio Bursts, including duty factors, time scales and repetition. The sudden release of magnetic energy in a neutron star magnetosphere, as in popular models of SGR, can meet the energy requirements of FRB but requires both the presence of magnetospheric plasma in order that dissipation occur in a transparent region and a mechanism for releasing much of that energy quickly. FRB sources and SGR are distinguished by long-lived (up to thousands of years) current-carrying coronal arches remaining from formation of the young neutron star, and their decay ends the phase of SGR/AXP/FRB activity even though "magnetar" fields may persist. Runaway increase in resistance when the current density exceeds a threshold releases magnetostatic energy in a sudden burst and produces high brightness GHz emission of FRB by a coherent process; SGR are produced when released energy thermalizes as an equlibrium pair plasma. Failures of some alternative FRB models and the non-detection of SGR 1806-20 at radio frequencies are discussed in appendices.

*Subject headings:* radio continuum: general — plasmas — radiation mechanisms: non-thermal — gamma rays: general

## 1. Introduction

Fast Radio Bursts (FRB) and Soft Gamma Repeaters (SGR) are rare and brief episodic events. Many authors (Popov & Postnov 2007, 2013; Kulkarni, *et al.* 2014; Lyubarsky 2014; Kulkarni, Ofek & Neill 2015; Pen & Connor 2015; Katz 2016) have noted this similarity and have suggested that FRB and SGR may be associated. This paper considers the physical processes that may make FRB from the sudden releases of magnetic energy that are believed to power SGR. FRB are, even at "cosmological" distances, $\sim 10^{-4}$ as powerful as the most powerful SGR, so a process that makes FRB from SGR need not be efficient.

The recent discovery (Masui, *et al.* 2015) of linear polarization and Faraday rotation in one FRB strengthens the case for cosmological distances. The measured rotation measure of FRB

110523 was $-186$ rad/m$^2$, implying the line-of-sight integral

$$\int n_e B_\parallel \, d\ell = 229 \text{ pc } \mu\text{G cm}^{-3}. \quad (1)$$

Comparing to its dispersion measure of 623 pc cm$^{-3}$ yields the electron density-averaged parallel field along the line-of-sight

$$\langle B_\parallel \rangle_{n_e} \equiv \frac{\int n_e B_\parallel \, d\ell}{\int n_e \, d\ell} = 0.37 \ \mu\text{G}. \quad (2)$$

This is more than an order of magnitude less than typical spiral galaxy fields $\sim 10\,\mu$G (Widrow 2002), and several orders of magnitude less than plausible fields in dense clouds or the immediate environments of stars. It indicates that the overwhelming majority of the dispersion occurs in the intergalactic medium where nanogauss or weaker fields are expected, and confirms the inference of "cosmological" distances. This implies that FRB may have powers as great as $10^{43}$ erg/s (Thornton, *et al.* 2013), and requires correspondingly energetic sources. SGR, observed to have powers as high as $10^{47}$ erg/s (Hurley, *et al.* 2005), can satisfy this requirement.

It is generally accepted (Katz 1982; Thompson & Duncan 1992, 1995; Katz 1996) that SGR outbursts result from the dissipation of magnetostatic energy in the magnetosphere of a highly magnetized neutron star (the "magnetar" model). Thompson & Duncan (1995) suggested that the rare giant flares of SGR are produced by a rupture propagating across the entire solid crust, the general failure of a brittle object found in a model of brittle fracture (Katz 1986; Bak, Tang & Wiesenfeld 1987) now called "self organized criticality".§2 presents the phenomenological case for associating SGR with FRB. In §3 I apply the well-known theory of long-lived coronal currents in SGR to FRB. These currents are relics of neutron star formation, and their lifetimes are consistent with the inferred ages of SGR and indicate that FRB are similarly young. The presence of such magnetospheric currents distinguishes these magnetars from neutron stars in which currents are confined to the dense interior. §4 estimates the energy to which electrons are accelerated, which determines the decay time of the magnetospheric currents. §5 suggests a possible outburst mechanism and §6 considers curvature radiation as the emission mechanism of FRB, estimating the required charge clumping factor. §7 is a brief summary and conclusion. Appendix A considers the hypothesis that Compton recoil of pair annihilation radiation may produce a plasma instability in the irradiated plasma, leading to large amplitude plasma waves that might produce high brightness GHz radiation; this hypothesis fails on energetic grounds. Appendix B considers some alternatives to the SGR hypothesis for FRB at cosmological distances, specifically giant pulsar pulses and neutron star collapse, and finds them wanting. Appendix C discusses the non-detection of a FRB in a radio observation (Tendulkar, Kaspi & Patel 2016) fortuitously simultaneous with the giant outburst of SGR 1806-20, and suggests possible explanations.

## 2. The Case for Associating SGR and FRB

FRB and SGR have three distinct similarities that suggest an association:

1. Duty Factor: Their duty factors, defined $D \equiv \langle F(t)\rangle^2/\langle F(t)^2\rangle$, where $F(t)$ is the flux, quantify the the fraction of the time in which a source emits at close to its peak flux, are extremely low: $D \sim 10^{-10}$ for SGR and $D < 10^{-8}$ for at least one FRB (Law, *et al.* 2015).

2. Time scale: The intrinsic durations of FRB have not been measured but Thornton, *et al.* (2013) found instrumentally-limited upper bounds of about 1 ms for several FRB. Some other FRB have had widths up to $\approx 10\,$ms that are attributed, because of their $\propto \nu^{-4}$ frequency dependence, to broadening by multipath propagation, and only upper bounds can be placed on the intrinsic pulse widths. This is consistent with the rise times of giant SGR outbursts: The rise time of the March 5, 1979 outburst of SGR 0525-66 was $< 200\,\mu$s (Cline 1980; Cline, *et al.* 1980), Palmer, *et al.* (2005) reported an exponential rise time of $300\,\mu$s for the giant December 27, 2004 outburst of SGR 1806-20, while their published data suggest a value of $200\,\mu$s, and the giant August 27, 1998 flare of SGR 1900+14 had a rise time of $< 4\,$ms (Hurley, *et al.* 1999) and earlier outbursts had rise times $\leq 8\,$ms (Mazets, Golenetskii & Gur'yan 1979). These time scales are shorter than those of any other known astronomical event except gravitational wave emission by coalescing black holes and the pulses and subpulses of some pulsars; GRB durations and subpulse time scales are all $\gtrsim 30\,$ms (Fishman, *et al.* 1994; Qin, *et al.* 2013).

3. Repetition: SGR repeat in complex irregular patterns, with periods of activity interspersed in longer periods of quiescence. The double pulse of FRB 121002, with subpulses separated by about 2 ms (Thornton 2013; Champion, *et al.* 2015) may be considered a repetition, and multiple repetitions of FRB 121102 were recently discovered (Spitler, *et al.* 2016), with irregular spacings reminiscent of the activity of SGR 1806-20 (Laros, *et al.* 1987). FRB are not catastrophic events that destroy their sources, and resemble SGR rather than GRB.

## 3. The Magnetosphere

It was realized soon after the discovery of the first SGR 0525-66 in 1979 that its combination of rapid rise ($< 200\,\mu$s) and energy release of $10^{44}$–$10^{45}$ ergs (Cline 1980; Cline, *et al.* 1980) required a source in a region of high energy density. Magnetic reconnection (Priest & Forbes 2000) in the magnetosphere of a neutron star with (then) unprecedentedly strong magnetic fields was a natural model for the energy source (Katz 1982; Thompson & Duncan 1992, 1995).

In magnetic reconnection magnetic energy is dissipated by resistive heating or particle acceleration in thin current sheets separating regions of differing, but comparatively homogeneous, magnetic fields. The current sheets may be modeled as resistors in series with an inductive energy store. If the electric field in the current sheets is large enough, counterstreaming electrons and ions (or positrons if they are present) make the plasma unstable to a variety of plasma waves. Correlated particles ("clumps") become effective scatterers, a condition described by an "anomalous" resistivity. This anomalous resistivity may be many orders of magnitude greater than the nominal resistivity resulting from interactions with uncorrelated particles.

The explosive growth of the resistivity $\rho_e$ as a plasma instability exponentiates, while the current is held nearly constant by the circuit inductance, implies a proportionally explosive growth of the electric field $\vec{E} = \rho_e \vec{J}$ and of the dissipation rate $\vec{E} \cdot \vec{J} = \rho_e J^2$ (in large magnetic fields $\rho_e$, written here as a scalar, is a tensor, complicating the problem but not changing the qualitative conclusion). The result can be rapid dissipation of large amounts of magnetostatic energy, depending on the evolution of $\rho_e$ in space and time.

At energy fluxes $\gtrsim 10^{29}$ ergs/cm$^2$-s, such as observed in giant SGR flares, the energy released thermalizes into an opaque equilibrium pair-black body photon gas, and a black body spectrum with temperature $\sim 20$ keV is emitted (Katz 1996), roughly consistent with observed SGR spectra. Confinement of the charged particles by the magnetic field (Katz 1982; Thompson & Duncan 1995; Katz 1996) permits the radiated intensity to exceed the Eddington limit by large factors, as observed. Equilibration is expected during most of the $\sim 0.1$ s duration of giant SGR flares. Their initial $< 1$ ms rise times may correspond to the progress of a reconnection wave along a current sheet as plasma instability produces large amplitude charge clumps and increases resistivity by orders of magnitude.

Some positrons escape their source and annihilate in dense cooler matter such as the neutron star's surface, emitting characteristic annihilation radiation at energies about 511 keV, as reported from SGR0525-66 (Cline 1980; Cline, *et al.* 1980). It is natural to associate the $< 1$ ms FRB with the $< 1$ ms rise time of giant SGR flares, before the electron-positron pairs have had time to equilibrate as a lower temperature plasma, converting most of their rest mass energy into black body photons.

Idealized neutron stars have sharply defined radii, with thermal scale heights $\lesssim 1$ cm after rapid early cooling. Above this scale height (unless they are accreting) the surrounding space is nearly vacuum, filled only with a non-neutral plasma with the Goldreich-Julian density (Davis 1947; Hones & Bergeson 1965; Goldreich & Julian 1969)

$$n_{GJ} = -\frac{\vec{\omega}_{rot} \cdot \vec{B}}{2\pi ce} \tag{3}$$

for an aligned magnetic dipole field and rotation rate $\omega_{rot}$. The defining characteristic of "magnetar" models is the assumption that rotation is unimportant: their radiation is derived from their magnetostatic energy, $n_{GJ}$ is insignificant and (except for rotational modulation of the observed radiation) the star may be considered non-rotating.

This leads to questions for magnetar models of FRB: Magnetic reconnection is implausible in the neutron star interior whose high density implies high conductivity and low electron-ion drift velocity. This precludes plasma instability and the development of anomalous (turbulent) resistivity, the generally accepted mechanism of magnetic reconnection (Priest & Forbes 2000) in low density plasma. If reconnection were somehow to occur in the neutron star interior it would only warm the dense matter there, with the released energy slowly diffusing to the surface to be radiated as thermal X-rays.

The electron-ion drift speed

$$v_{drift} = \frac{J}{n_e e} \sim \frac{Bc}{4\pi r n_e e} \sim 10^4 \frac{B_{15}}{\rho_m} \text{ cm/s}, \tag{4}$$

where $\rho_m$ is the mass density and $B_{15} \equiv B/(10^{15}\text{G})$. Anomalous resistivity can only occur where $\rho_m \ll 1\,\text{g/cm}^3$, in an optically thin atmosphere (that may not exist if magnetic quantization of electron states gives neutron stars abrupt surfaces).

Rapidly rising SGR outbursts and FRB must occur in nearly transparent regions (optical depth $\lesssim 1$) in order that their radiation escape in their observed sub-ms rise times. Yet reconnection cannot occur in a vacuum magnetosphere, despite its high magnetostatic energy density, because no currents flow in vacuum. Here the theory (Thompson & Duncan 1992, 1995; Thompson, Lyutikov & Kulkarni 2002; Beloborodov & Thompson 2007) of the magnetar origin of SGR is applied to SGR models of FRB.

These problems may be resolved if substantial portions of the neutron star's magnetic moment are produced by current loops flowing through long-lived quasi-neutral coronal arches above the high density neutron star surface. Actual force-free configurations (in magnetar fields the cross-field conductivity is very small, electrons are in their quantized ground states and any cross-field currents would imply enormous Lorentz forces, so that $\vec{J} \parallel \vec{B}$) are complex (Parker 1979; Akgün, *et al.* 2016).

As a neutron star forms from the collapse of a stellar core, frozen-in magnetic fields are amplified by compression and possibly by turbulence. In the earlier stages of contraction the matter pressure far exceeds the magnetic stress. Currents flow along the field lines, along which the conductivity is always higher than perpendicular to them (although at high densities there may also be cross-field currents). As the matter, radiating neutrinos, gradually settles into its final configuration, the magnetic stress becomes dominant in the low density regions above the developing neutron star surface, and the matter there is constrained to flow along the field lines. Magnetic field lines still penetrate that surface (if they didn't, all multipole moments would be zero). The magnetosphere must be force-free, with $\vec{J} \parallel \vec{B}$, because pressure gradients are insufficient to oppose any Lorentz force and because the cross-field conductivity is low at low matter density. However, there is no reason to expect the parallel component of $\vec{J}$ to disappear during collapse.

The resulting picture is one of a magnetosphere in which, near the stellar surface

$$J \sim \frac{cB}{4\pi r} \sim 2 \times 10^{18} B_{15} \frac{\text{esu}}{\text{cm}^2\text{s}}, \tag{5}$$

where $B_{15}$ refers only to that portion of the field generated by magnetospheric currents.

Current flows on loops, and produces a magnetic flux through a representative loop

$$\Phi \sim Br^2 \sim 10^{27} B_{15} \text{ G-cm}^2. \tag{6}$$

Magnetospheric current loops of this sort have been considered by Thompson, Lyutikov & Kulkarni (2002); Beloborodov & Thompson (2007); Beloborodov (2009) as the origin of magnetar coronæ

and by Lyutikov (2006, 2013) to explain SGR flares and magnetar "anti-glitches" if they open to infinity during flares, in analogy to Solar coronal mass ejections.

The electromotive force (EMF) induced by the changing flux through the loop drives the current flow along the magnetic field lines At one foot of the arch electrons are pulled out of the surface plasma and accelerated towards the other foot; positive ions (and possibly positrons) are pulled from the surface and accelerated in the opposite direction. Both signs of charge carriers contribute to the current. Beloborodov & Thompson (2007) assumed only one positive charge carrier (or positive charge carriers all with the same charge to mass ratio) and found that no steady solution is possible and that pairs must be produced, but multiple positive ion species and ionization states are likely to be present. Our estimates average over any rapid variability, whose time scale is $\sim r/c \sim 30\,\mu$s, shorter even than SGR rise times and the upper bounds on FRB duration.

The current is mostly carried by relativistic electrons with density

$$n_e \sim \frac{J}{(1+J_+/J_-)ce} \sim \frac{B}{4\pi re} \sim 2\times 10^{17} B_{15}\ \mathrm{cm}^{-3}, \tag{7}$$

where $J_+$ and $J_-$ are the current densities of positive and electron charge carriers, respectively; $J_+/J_- \leq 1$ because ions move more slowly than electrons. The electrons in the current loop must be quasi-neutralized by ions or positrons because otherwise their electrostatic field $E \sim n_e e r^3/r^2 \sim B/4\pi$ would be impossibly large.

This electron density may be compared to the co-rotation density (Eq. 3): $n_{GJ}/n_e < 2\omega_{rot} r/c$. The co-rotating charge density is insignificant except near the co-rotation radius, where the magnetic energy density and available power are very small.

The quasi-neutral low density current-carrying plasma is gravitationally attracted to the star, and would slide down the magnetic field lines to the surface. However, $n_e$ cannot fall below the value given by Eq. 7 because that would interrupt the flow of current, changing the flux through the loop and inducing an EMF sufficient to maintain the current.

The current-carrying electrons strike the star with a Lorentz factor $\gamma$, acquired in their descent from the top of the loop by the electric field that lifts positive ions to maintain quasi-neutrality. The implied EMF is $\approx \gamma m_e c^2/e$ because contributions from the electric field lifting the electrons and inside the star are small (electrons require little gravitational energy to lift and the stellar interior is an Ohmic conductor of high conductivity). Equating this EMF to $\partial\Phi/\partial(ct) \sim \Phi/c\tau \sim Br^2/c\tau$ yields the magnetic decay time $\tau$:

$$\tau \sim \frac{r^2 eB}{\gamma m_e c^3} \sim 6\times 10^5 \frac{B_{15}}{\gamma}\ \mathrm{y}. \tag{8}$$

Of course, only the component of field attributable to magnetospheric current decays on this time scale.

The ratio Age/$B$, where Age is the spin-down age, is plotted in Fig. 1 for pulsars from the ATNF Pulsar Catalogue (Manchester, *et al.* 2005). This provides an estimate of $\gamma$ for SGR/AXP for

which the magnetospheric current contributes a substantial fraction of the slowing-down torque, but it has no such significance for ordinary radio pulsars whose magnetospheric currents have decayed. Pulsars categorized in the Catalogue as "radio but not AXP" are indicated as "Radio" while those categorized as "AXP" are indicated as "AXP" or (the three with observed giant flares) "SGR". Pulsars with smaller estimated fields (including most ordinary pulsars as well as millisecond pulsars) are not shown. It is likely that each category contains some incorrectly classified objects (*e.g.,* accreting neutron stars or other X-ray pulsars misclassified as AXP in the Catalogue).

The horizontal lines are upper bounds on the actual ages corresponding to the indicated values of $\gamma$. If the actual ages are close to the spindown ages, as is the case for pulsars that have spun down from much faster rotation at birth, then SGR/FRB will lie on or below the lines corresponding to their values of $\gamma$. They will be below these horizontal lines if their magnetospheric currents have decayed very little, possibly suggesting that the neutron star is in the early stages of its active life as a SGR/FRB. If its spindown age is greater than its actual age, a neutron star may lie above the horizontal line; however, the absence of points in the upper right part of the figure suggests that this is not common.

All radio pulsars lie above the $\gamma = 20$ line, suggesting that when SGR reach the age $\tau$ they turn into radio pulsars even if their fields remain in the "magnetar" range. This is consistent with the hypothesis that SGR must be younger than $\tau$, and that any older object can only be a radio pulsar, however large its magnetic field. Every "AXP" in the Catalogue above the $\gamma = 20$ line has $B \leq 2.2 \times 10^{14}$ G (indicated by a dashed line), and every "AXP" with $B \leq 2.2 \times 10^{14}$ is above the $\gamma = 20$ line. This 1:1 correspondence suggests that these objects form a population distinct from those of the higher-B, younger-aged "AXP", and may not be SGR/AXP at all.

The concentration of the SGR with giant flares to the lower right corner of Fig. 1 appears to be statistically significant. Of the five "AXP" below the $\gamma = 100$ line, three are the SGR with giant flares ($P = 0.024$) and these three are among the four "AXP" with the highest Age/$B$ ($P = 0.011$). Although these statistics are *a posteriori*, they suggest that as SGR age past $\tau$ they may remain AXP as a result of magnetic dissipation within their interiors, but that their SGR activity decays along with their magnetospheric currents. Only a fraction of AXP are SGR, and the absence of SGR activity in most AXP (those with greater ratios of age to field) is not an artefact of limited observations but an intrinsic property.

## 4. Electron Energy

For a magnetic arch with a gravitational potential difference $\Omega$ between its top and the neutron star surface,

$$\int_A^C \vec{E} \cdot d\vec{\ell}_{arch} = \Omega \frac{A m_p}{Ze} \sim \frac{GMm_p \delta r}{r^2 e} \frac{A}{Z} \tag{9}$$

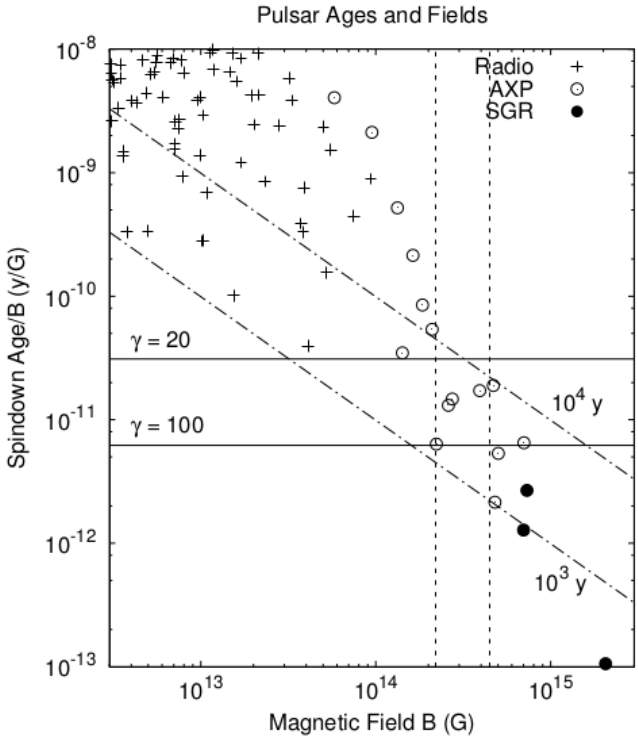



Fig. 1.— Spindown ages and magnetic fields of all objects in the ATNF Pulsar Catalogue (Manchester, *et al.* 2005) with parameters in the displayed range that are categorized as "radio but not AXP" or "AXP". Of the "AXP", only four (all with $2 \times 10^{14} < B < 3 \times 10^{14}$) have reported radio emission. The SGR that have shown giant flares (SGR 0526-66, SGR 1806-20 and SGR 1900+14) are categorized as "AXP" but here shown with a distinctive symbol. Diagonal dot-dashed lines indicate spindown ages. Horizontal lines indicate the ratio of lifetime to $B$ (plotted on the "Spindown Age/B" axis) corresponding to their value of $\gamma$. All "AXP" lying below the $\gamma = 20$ line have $B > 2.2 \times 10^{14}$ G and all below the $\gamma = 100$ line have $B > 4.5 \times 10^{14}$ G; these fields are indicated by vertical dashed lines.

is required to raise the neutralizing ions from A to the top of the arch (C) a height $\delta r$ above the neutron star's surface, where the atomic number $A$, proton mass $m_p$ and ionization state $Z$ describe the neutralizing ions. The electrons, closing their path to the stellar surface, acquire a kinetic energy $-e\int_C^A \vec{E}\cdot\vec{d\ell}_{arch}$ that they dissipate in collisions in the star at A.

Above the surface of a cooling neutron star with a nominal surface black body temperature of $\sim$ 0.1–1 keV iron may be $\sim$ 20–24 times ionized, although less in strong magnetic fields that increase the ionization potentials. The plausible range of $A/Z$ is from 1 (accreted hydrogen) to $\sim$ 2–5 for strongly magnetized iron.

The magnetostatic energy available (in a dipole field) is $B^2R^3/6$ (Katz 1982) and the dissipated power is $B^2R^3/(6\tau) \sim 10^{34}B_{15}\gamma$ ergs/s if the neutron star is young enough that much of its magnetic moment is produced by currents in loops that extend through the surface into the magnetosphere. After those loops decay, the stars will retain the magnetic moments produced by their internal currents. The same result is obtained, to order of magnitude, from Eq. 5 if $J$ is assumed to extend over the entire surface:

$$P \sim 4\pi r^2 n_e \gamma m_e c^3 \sim \frac{Br\gamma m_e c^3}{e} \sim 6\times 10^{34}\gamma B_{15}\ \mathrm{ergs/s}, \tag{10}$$

consistent with the steady (except for rotational modulation) X-ray emission from the heated surface. This power is in addition to that generated by magnetic dissipation in the stellar interior.

Equating the EMF (Eq. 9) to $\gamma m_e c^2/e$ and taking $\delta r = 3\,\mathrm{km}$,

$$\gamma \approx \frac{\Omega}{c^2}\frac{m_p}{m_e}\frac{A}{Z} \approx 40\frac{A}{Z}, \tag{11}$$

with $\gamma$ plausibly in the range 40–400. Substituting this into Eq. 8 yields

$$\tau \sim \frac{r^2 eB}{m_p c\Omega}\frac{Z}{A} \sim 5000\ B_{15}\left(\frac{\delta r}{3\,\mathrm{km}}\right)^{-1}\frac{Z}{A}\ \mathrm{y}. \tag{12}$$

## 5. Outburst Mechanism

### 5.1. Plasma Instability?

The counterstreaming electron and ion currents would seem to invite the two-stream plasma instability (Chen 1974). This is unlikely to explain the outbursts:

1. The plasma frequency corresponding to the electron density of Eq. 7 exceeds observed FRB frequencies by orders of magnitude, even allowing for the relativistic increase of mass with the Lorentz factor (11), so that oscillations of this plasma cannot emit the observed radiation.

2. The counter streaming currents are present at all times. An instability might produce steady emission, but there is no evident mechanism for it to make rare, low duty factor, giant outbursts.

3. The electrons are highly relativistic, moving with Lorentz factors $\gamma \gg 1$ exactly parallel to $\vec{B}$ because their transverse motion decays immediately in a quantizing magnetic field. Their response to the electric field of a longitudinal plasma wave with $\vec{E} \parallel \vec{B}$ is reduced by a factor $\gamma^{-3}$ compared to that of nonrelativistic electrons (their response to any transverse component of $\vec{E}$ is zero because the magnetic field is quantizing). This suppresses the growth of the two-stream instability (Melrose & Yuen 2016).

### 5.2. Coulomb Scattering

The scattering cross-section of the neutralizing ions for the current-carrying electrons may be estimated, though a quantitative calculation would require use of their wave-functions in the quantizing magnetic field. We assume that the electron motion is only parallel to the field and that the backscattering cross section is the integral of the Mott cross-section in the relativistic limit, ignoring ionic recoil (ionic transverse motion is less strongly quantized even in "magnetar" fields), over the backward hemisphere:

$$\begin{aligned} \sigma &= 2\pi \int_{-1}^{0} \frac{Z^2 e^4}{4\gamma^2 m_e^2 c^4} \csc^4(\theta/2) \cos^2(\theta/2)\, d\cos\theta \\ &= \pi(1-\ln 2)\frac{Z^2 e^4}{\gamma^2 m_e^2 c^4} = 7.6\times 10^{-26}\frac{Z^2}{\gamma^2}\ \mathrm{cm}^2. \end{aligned} \tag{13}$$

Using the estimate (11) for $\gamma$

$$\sigma \sim 5\times 10^{-29}\frac{Z^4}{A^2}\ \mathrm{cm}^2 \lesssim 7\times 10^{-27}\ \mathrm{cm}^2, \tag{14}$$

where the upper bound is taken for completely ionized Fe ions.

The integrated column density of electrons along a coronal arch of length $r$ is

$$n_e r \sim \frac{B}{4\pi e} \sim 2\times 10^{23} B_{15}\ \mathrm{cm}^{-2}. \tag{15}$$

Assuming the current-carrying electrons are quasi-neutralized by ions (see below), the corresponding column density of ions is

$$n_i r = \frac{n_e r}{Z} \sim \frac{B}{4\pi e Z} \sim 2\times 10^{23}\frac{B_{15}}{Z}\ \mathrm{cm}^{-2}. \tag{16}$$

Comparing to the cross-section (16) shows that the ionic Coulomb scattering probability $P_{scatt}$ of the current-carrying electrons in the magnetospheric arch is negligible:

$$\begin{aligned} P_{scatt} = n_i r\sigma &\sim \frac{Z^2 e^4}{\gamma^2 m_e^2 c^4}\frac{B}{4\pi e Z} \sim \frac{1-\ln 2}{4} B\frac{Z^3 e^3}{\Omega^2 m_p^2 A^2} \\ &\sim \frac{1-\ln 2}{4}\frac{m_e^2 c^4}{\Omega^2 m_p^2}\alpha\frac{B}{B_c}\frac{Z^3}{A^2} \sim 3\times 10^{-7}\frac{Z^3}{A^2}\frac{B_{15}}{\Omega_{20}^2} \ll 1, \end{aligned} \tag{17}$$

where $B_c \equiv m_e^2 c^3/e\hbar = 4.413 \times 10^{13}$ G is the quantum critical field, $\alpha$ is the fine-structure constant and $\Omega_{20} \equiv \Omega/(10^{20}\,\mathrm{ergs/g})$. The electrons are ballistically accelerated by the electrostatic field that supports the neutralizing ions, and Ohmic resistivity is inapplicable.

### 5.3. A Possible Mechanism

Crustal and interior motions in the neutron star rearrange its surface magnetic field and the structure of its magnetosphere (Thompson & Duncan 1992, 1995). As a result, the current may, locally or globally, concentrate on sheets of thickness $h \ll r$. Concentration of currents on thin sheets occurs during magnetic reconnection (Priest & Forbes 2000). When contacting plates of highly conductive neutron star crust, with frozen-in fields, are displaced with respect to one another, volumes of magnetosphere with different fields may be brought into contact, with the tangential magnetic discontinuity accommodated by a thin current sheet. In Eqs. 5 and 7 $r$ is replaced by $h$ which may be very small, at least near the crustal plates. Eq. 17 becomes

$$\begin{aligned} P_{scatt} &\sim \frac{1-\ln 2}{4}\frac{m_e^2 c^4}{\Omega^2 m_p^2}\alpha\frac{Z^3}{A^2}\frac{B}{B_c}\frac{r}{h} \\ &\sim 3\times 10^{-7}\frac{Z^3}{A^2}\frac{B_{15}}{\Omega_{20}^2}\frac{r}{h}. \end{aligned} \tag{18}$$

When $P_{scatt} \ll 1$ the resistivity is not Ohmic; most electron motion is ballistic. But when $P_{scatt} \gg 1$ the "scattering optical depth" of the coronal arch to the electrons is $P_{scatt}$ and the electrons undergo a one-dimensional random walk (the only scattering possible is in the backward direction), reducing their mean speed to $c/P_{scatt}$. This increases the charge density required to carry the current density by the same factor of $P_{scatt}$, and quasi-neutrality multiplies the density of scatterers by that factor again. The result is a limiting current density set by the condition $P_{scatt} \approx 1$:

$$\begin{aligned} J_{max} &\sim \frac{\Omega^2 m_p^2 c}{\pi(1-\ln 2)e^3 r}\frac{A^2}{Z^3} \sim 8\times 10^{24}\ \Omega_{20}^2\frac{A^2}{Z^3}\ \frac{\mathrm{esu}}{\mathrm{cm^2\text{-}s}} \\ &\sim 3\times 10^{15}\ \Omega_{20}^2\frac{A^2}{Z^3}\ \frac{\mathrm{A}}{\mathrm{cm^2\text{-}s}}. \end{aligned} \tag{19}$$

When the current density required by the magnetic field exceeds $J_{max}$

$$\frac{c}{4\pi}\frac{B}{h} > J_{max} \tag{20}$$

a condition found if

$$\frac{h}{r} < \frac{1-\ln 2}{4}\frac{Be^3}{\Omega^2 m_p^2}\frac{Z^3}{A^2} \sim 3\times 10^{-7}\frac{B_{15}}{\Omega_{20}^2}\frac{Z^3}{A^2}. \tag{21}$$

it becomes impossible for the current sheet to carry the current implied by the assumed magnetic configuration. It is difficult to be sure what the consequences will be, but it is plausible that the

result will be a runaway increase in plasma density on the current sheet as the scattering and resistance increase and the rapid deposition of enough magnetic energy and the field configuration relaxes to one consistent with $J < J_{max}$.

## 6. The Clumping Factor

The extraordinary brightness of FRB requires coherent emission. Katz (2014) estimated the degree of clumping for emission by relativistically expanding plasma, but in the present model the source is trapped in a neutron star magnetosphere, with zero bulk velocity. The angle-integrated spectral density emitted by a charge $N_e e$ moving with Lorentz factor $\gamma \gg 1$, integrated over the passage of its radiation pattern, is (Jackson 1962)

$$\frac{dI}{d\omega} \sim \frac{(N_e e)^2 \gamma}{c}. \tag{22}$$

Adopting $\gamma = 100$, distributing the observed $\sim 10^{40}$ ergs of the brightest FRB (Thornton, *et al.* 2013) over a spectral bandwidth $\sim 10^{10}$ s$^{-1}$ and $\sim 10^{10}$ radiating "bunches" (coherent emission is only possible for sources whose dimensions are $< \lambda/2 \approx 10\,\mathrm{cm}$) and allowing for $\sim 1\,\mathrm{ms/(r/c)} \sim 30$ passages through a current sheet of dimension $\sim r$ yields $N_e \sim 6 \times 10^{22}$.

This would imply a potential $V \sim N_e e/(\lambda/2) \sim 3 \times 10^{12}\,\mathrm{esu}$, or an electrostatic energy of $1.5 \times 10^3$ ergs ($10^6$ GeV) per electron ($\gamma \sim 10^9$) and an electric field of $3 \times 10^{11}\,\mathrm{cgs}$ or $10^{14}$ V/cm. Such an electric field would be about 1% of the characteristic quantum field $E_c \equiv m_e^2 c^3/e\hbar$ (Heisenberg & Euler 1936; Schwinger 1951), approaching the threshold of "Schwinger sparks" at 5% of the characteristic field (Stebbins & Yoo 2015). However, these fields are inconsistent with the assumed $\gamma \sim 100$.

A self-consistent solution of Eq. 22 and $\gamma m_e c^2 = N_e e^2/(\lambda/2)$ is

$$\begin{aligned} N_e &= \left(\frac{dI}{d\omega}\frac{(\lambda/2)m_e c^3}{e^4}\right)^{1/3} \sim 2 \times 10^{20} \\ \gamma &\sim 10^7. \end{aligned} \tag{23}$$

The electron energy $eV \sim 10^4$ GeV, about 100 times less than in the preceding paragraph.

These extraordinary numbers follow from the inferred brightness temperatures (and cosmological distances) of FRB and are not specific to the model (Katz 2014); qualitatively similar inferences follow from the observation of nanosecond "nanoshots" of Galactic pulsars (Soglasnov, *et al.* 2004; Hankins & Eilek 2007) whose sources must be as small as a few m. Such electrostatic potentials imply much larger $\gamma \sim eV/(m_e c^2)$ during outburst than are found for the slowly decaying, quasi-steady state magnetosphere in §4.

The plasma frequency at the electron density (7) exceeds the frequency of the observed radiation, and in a current sheet carrying the current density (19) it is orders of magnitude greater

still. Despite this, it is possible for radiation at the observed frequencies to be emitted because the dense plasma, and radiation source, is confined on magnetic surfaces with an abrupt density discontinuity; surface charges and currents of this overdense plasma are the sources of radiation, which does not propagate through the plasma itself.

Curvature radiation has been suggested as the emission mechanism of radio pulsars (Ghosh 2007; Melrose & Yuen 2016), with their high brightness temperature requiring, and explained by, clumping (correlation) of the radiating electrons. Curvature radiation may also explain their linear and circular polarization (Gil & Snakowski 1990; Ganjadhara 2010; Kumar & Ganjadhara 2012; Wang, Wang & Han 2014). The subject remains controversial.

In analogy, curvature radiation might account for the radio emission of FRB. An argument in favor of this hypothesis is the observation of both linear (Masui, *et al.* 2015) and circular (Petroff, *et al.* 2015) polarization in FRB, though in different events. However, at the Lorentz factors estimated during outburst (23), curvature radiation would occur at frequencies far in excess of those observed in FRB.

## 7. Summary and Conclusion

Several lines of argument, including energetics, comparison of event rates with those of other transients such as SNR and GRB, and the energy emitted as an accreting or despinning neutron star approaches its stability limit indicate that FRB are not produced by one-time catastrophic events. This conclusion is supported by the discovery (Thornton 2013; Champion, *et al.* 2015) of a double-pulsed FRB with subpulse separation (about 2 ms) greater than the neutron star collapse time, indicating two distinct events produced by the same source, and was recently confirmed by the discovery of a repeating FRB (Spitler, *et al.* 2016). In such models there is no connection between the observed FRB rate and the birth rate of their parent objects.

FRB may be associated with other brief transients. If FRB are at the "cosmological" distances indicated by their dispersion measures, giant PSR pulses (including RRAT) cannot be sufficiently energetic unless the neutron star is both extremely fast-rotating and strongly magnetized. This combination is not observed among Galactic pulsars and is almost self-contradictory, because strong magnetic fields lead to rapid spindown. The remaining category of known brief electromagnetic transients is the Soft Gamma Repeaters, and in particular the sub-ms rise times of their giant flares. The rate of Galactic giant SGR flares exceeds the observed rate of FRB per galaxy by about four orders of magnitude if FRB are at "cosmological" distances, but there are several possible explanations, of which the most obvious is that only a small fraction of SGR-associated FRB are energetic enough to be observable at those distances.

Consideration of possible mechanisms for dissipation of magnetostatic energy in transparent regions, as required by the fast (sub-ms) time scales of both FRB and the rising phase of giant SGR flares, points toward currents flowing on magnetospheric arches, analogous to Solar coronal

arches. Such arches have lifetimes of thousands of years or less, depending on the magnitude of the magnetic field, and may explain why SGR/AXP behavior is found in young, high-field neutron stars, and why neutron stars that are either older or have smaller fields may be radio pulsars but are not SGR/AXP. The criterion is the ratio of field to age, explaining why older neutron stars do not show SGR/AXP activity even if their fields are in the "magnetar" range (Manchester, *et al.* 2005), as well as younger but lower field neutron stars like the Crab pulsar.

I hypothesize that SGR/AXP and FRB activity require the persistence of magnetospheric currents. Their decay time $\tau$ (Eq. 12) for neutron stars with the highest magnetic fields is consistent with estimated SGR/AXP ages. The smaller values of $\tau$ for neutron stars with lower fields (such as the Crab pulsar) explain why they are not SGR/AXP, even if they are younger than observed SGR/AXP. Magnetospheric currents have also decayed in older pulsars, even those with fields in the "magnetar" range (McLaughlin, *et al.* 2003; Manchester, *et al.* 2005), explaining why they too are not SGR/AXP.

The fact that the event rate of FRB ($\sim 10^{-5}$/y per galaxy, if at cosmological distances), is $\sim 10^4$ times the observed rate of giant flares from Galactic SGR indicates that if they are associated, the association is with a tiny minority of SGR flares, perhaps the most energetic. SGR 1806-20 radiated about $4 \times 10^{46}$ ergs (Hurley, *et al.* 2005), and the rarer SGR associated with FRB at "cosmological" distances may be orders of magnitude more energetic. Hurley, *et al.* (2005) suggested that some short (duration $< 2$ s) GRB are actually SGR, but SGR flares are observed to have even shorter widths of 0.1–0.2 s, excluding them as the sources of most "short" GRB. The observed SGR may radiate from magnetically confined pair plasmas (Katz 1982; Thompson & Duncan 1992, 1995) at photospheric temperatures of $\sim 20$ keV (Katz 1996), while the more energetic FRB may produce relativistically expanding pair plasmas. Because of Doppler boosting the escaping radiation has energies comparable to the initial MeV temperature (Goodman 1986), suggesting a new class of ultra-hard, short and faint GRB coincident with FRB.

Some alternative hypotheses and the non-detection of a FRB accompanying SGR 1806-20 are discussed in the appendices. Beloborodov & Li (2016) recently identified the power (10) with the steady emission of magnetars.

## A. Compton Recoil of Annihilation Radiation

In the latter ($\gtrsim 1$ ms) part of a SGR flare its pair plasma thermalizes, radiating the characteristic soft SGR spectra, but during their rapid ($< 1$ ms) rising phase more energetic pair annihilation gamma-rays (a tiny fraction of the total energy radiated) may be produced, such as were reported from SGR 0525-66 (Cline 1980; Cline, *et al.* 1980). These gamma-rays Compton scatter in surrounding plasma, creating a broadly directed flow of semi-relativistic electrons whose distribution function peaks at the highest kinematically permitted energy. This excites the "bump-on-tail" plasma instability in a background plasma.

### A.1. Distribution Function

Annihilation radiation Compton scatters on non-relativistic plasma, producing a broad beam of recoiling electrons. In the simplest possible case the annihilation spectrum is monochromatic with $h\nu = m_e c^2 = 511\,\mathrm{keV}$, the target electron distribution is "cold", with negligible (compared to $c$) thermal velocities, the target is sufficiently distant from the source that the photons can be considered a directed beam and the effects of magnetic fields are ignored (valid if $B \ll m_e c^3/e\hbar = 4.4 \times 10^{13}\,\mathrm{gauss}$ and $B$ is parallel to the photon beam). The differential scattering cross-section is given by the Klein-Nishina formula (Bjorken & Drell 1964)

$$\frac{d\sigma}{d\Omega} = \frac{e^4}{2m_e^2 c^4}\left(\frac{\nu'}{\nu}\right)^2\left(\frac{\nu'}{\nu} + \frac{\nu}{\nu'} - \sin^2\theta\right), \tag{A1}$$

where the frequencies of the incident and scattered photons are $\nu$ and $\nu'$. Kinematics dictates a relation between the direction of the scattered electron and its energy

$$\nu' = \frac{\nu}{1 + (2h\nu/m_e c^2)\sin^2(\theta/2)}. \tag{A2}$$

Plasma instability depends on the component of electron velocity parallel to the wave vector of the plasma oscillation, so consider only the component of velocity parallel to the incident photon beam. The resulting distribution function of scattered electrons is shown in Fig. 2:

The distribution function $f(\theta, v)$ of scattered electrons evolves as a result of Coulomb drag on the much larger population of unscattered electrons and of ions. This is described by a Fokker-Planck equation

$$\frac{\partial f(\theta, v)}{\partial t} = S(\theta, v) - \frac{\partial}{\partial v}\left(\frac{dv}{dt} f(\theta, v)\right), \tag{A3}$$

where $S$ is the scattering source function and $dv/dt \propto \beta^{-2}\gamma^{-3}$ represents Coulomb drag (slowing by loss of energy to background plasma; Gould (1972)). In steady state this reduces to:

$$f(\theta, v) = C\beta^2\gamma^3 \int_{v'=v}^{\infty} S(\theta, v')\, dv', \tag{A4}$$

where $\beta \equiv v/c$ and $\gamma \equiv (1-\beta^2)^{-1/2}$. Here $\vec{v}$ is the velocity vector and $v$ the speed; $\theta$ remains constant during slowing (aside from a small amount of straggling), so $f(\theta, v)$ may be evaluated independently for each $\theta$ and the three-space speed projected onto the beam direction.

### A.2. Plasma Instability

A multipeaked electron distribution function $f(v_x)$, such as that shown in Fig. 2 with the addition of the thermal electron peak at small velocity (not in the Figure, that only shows the scattering source) is unstable to the electrostatic "bump on tail" instability. This instability is

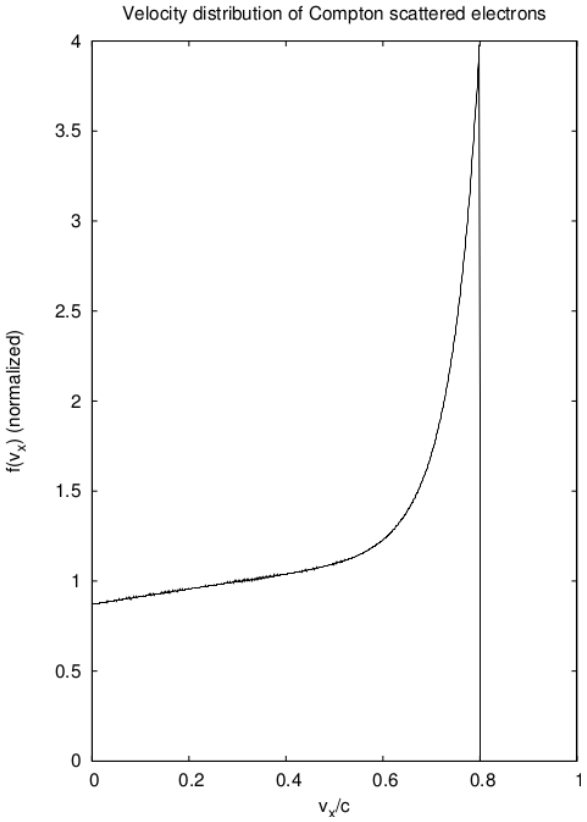



Fig. 2.— Normalized distribution function *vs.* velocity component in the beam direction of electrons Compton scattered by a beam of 511 keV photons.

essentially inverse Landau damping, and occurs whenever the derivative of the distribution function with respect to some component of electron velocity is positive. Electron plasma waves with phase velocities $v_{ph} = \omega/k$ ($\omega$ and $k$ are the plasma wave frequency and wave vector, related by the dispersion relation $\omega^2 = \omega_p^2 + 3k^2\lambda_D^2$ where $\omega_p$ is the plasma frequency and $\lambda_D$ the Debye length) for which $\partial F_0(v_x)/\partial v_x|_{v_x=v_{ph}} > 0$ grow at a rate (Chen 1974)

$$\gamma = \frac{\pi}{2}\frac{\omega_p^3}{k^2}\frac{n_{beam}}{n_e}\left.\frac{\partial F_0(v_x)}{\partial v_x}\right|_{v_x=\omega/k}, \tag{A5}$$

where $F_0(v_x)$ is the normalized one-dimensional electron distribution function of a density $n_{beam}$ of high velocity (Compton recoil) electrons and $n_e$ is the background electron density. If the fast electrons are only a small fraction of the total electron density and their speeds are much greater than the electron thermal velocity, conditions that are generally met, then for waves excited by the fast electrons $\omega \approx \omega_p$ and $k \approx \omega_p/v$, where $v$ is a velocity on the rising part of the electron distribution function. Then the growth rate becomes

$$\frac{\pi}{2}\frac{\omega_p v^2}{n_e}\left.\frac{\partial f(v_x)}{\partial v_x}\right|_{v_x=\omega/k}, \tag{A6}$$

where $f(v_x)$ is not normalized to $n_{beam}$ but is the full electron distribution function.

The rapid decrease of drag deceleration with increasing speed, shown by the factor $\beta^2\gamma^3$ in Eq. A4, acts to create a minimum in $f(v_x)$ (the large peak in $f(v_x)$ from thermal electrons at very small velocity is not shown in Fig. 2) even when $S(v)$ is a monotonically decreasing function, as it can be for power law photon spectra or a mixture of two- and three-photon annihilation (not shown). For example, if $S(v) \propto v^{-n}$, making the nonrelativistic approximation $\gamma \to 1$, then $f(v) \propto v^{3-n}$. For all but the most steeply decreasing $S(v)$, $n < 3$ and $f'(v) > 0$ for $v$ exceeding a few thermal velocities, and the plasma is unstable. In the opposite limit of scattering by very energetic gamma-rays $S(v) \to \delta(v-c)$, $f(v) \propto v^2\gamma^3$, $f'(v) > 0$ and again the plasma is unstable (for quantitative growth rates Eqs. A5, A6 need to be corrected for the relativistic increase in electron mass).

This mechanism of producing unstable electron distributions may operate anywhere an intense flux of gamma-rays, not necessarily from positron annihilation, whose spectrum is not too steep, is incident upon a non-relativistic plasma. The required intensity is determined by the competition between the growth rate $\gamma$ (Eqs. A5, A6), proportional to the gamma-ray flux, and the collisional damping rate of the plasma wave that depends on the plasma density and temperature.

For a plasma frequency comparable to the frequencies $\approx 1400\,\mathrm{MHz}$ of observed FRB, $n_{beam} \gtrsim 10^{-6} n_e$ is sufficient to grow the instability by $\sim 10$ $e$-folds to saturation in the sub-ms time scale of FRB.

### A.3. Energetic Failure

This apparently attractive model fails on energetic grounds. The total Klein-Nishina cross-section for a 511 keV photon is $2.85 \times 10^{-25}$ cm$^2$, so that annihilation radiation will penetrate a plasma to a depth of about $4 \times 10^{24}$ electrons/cm$^2$. If electrons receive an average energy of $m_e c^2$ the total deposited energy is about $3 \times 10^{18}$ ergs/cm$^2$. If more energy were deposited the electron thermal energies would be $\gtrsim m_e c^2$, their distribution function would not be inverted ($\partial f(v_x)/\partial v_x$ would be negative at all $v_x$) and there would be no instability. Over a hemisphere of a neutron star the total deposited energy must be less than $10^{31}$ ergs, failing to account for observed FRB energies, even assuming perfectly efficient radiation, by nine orders of magnitude.

An even stronger conclusion results from noting that the critical density for the observed 1.4 GHz FRB radiation, above which it cannot propagate, is $n_e = 2.4 \times 10^{10}\,\mathrm{cm}^{-3}$. A magnetosphere filled with that density of semi-relativistic plasma would contain less than $10^{23}$ ergs of plasma energy.

## B. Possible Alternatives to SGR?

A number of alternative sites of FRB have been considered, in most cases without detailed modeling of the emission mechanisms. Here I discuss two such sites that, like SGR, involve neutron stars, and point out significant unresolved questions.

### B.1. Giant pulsar pulses

The "nanoshots" of a few radio pulsars are even shorter than FRB, with durations of nanoseconds (Soglasnov, *et al.* 2004; Hankins & Eilek 2007), but involve energies smaller than those of FRB by many orders of magnitude. In fact, their instantaneous radiated power, even during their nanosecond peaks, is less than their pulsars' mean spin-down power. This supports the hypothesis that, as in classical pulsar theory (Gold 1968; Goldreich & Julian 1969; Ghosh 2007), they do not tap stored magnetic energy.

Giant pulsar pulses have been suggested (Connor, Sievers & Pen 2015; Cordes & Wasserman 2016) as the origin of FRB. If their instantaneous power is less than their mean spin-down power (no release of stored magnetostatic energy), as is always the case for Galactic radio pulsars, then the inferred luminosity of at least one FRB at "cosmological" distances ($L_{FRB} \gtrsim 10^{43}$ erg/s; Thornton, *et al.* (2013)) precludes explaining FRB as giant pulsar pulses unless the neutron stars are rotating near breakup and are very strongly magnetized and hence very young. Their ages must be $< E_{rot}/L_{FRB} \sim 100\,\mathrm{y}$, where $E_{rot} \approx 5 \times 10^{52}$ ergs is the rotational energy of a neutron star at its rotational limit. If intrinsic FRB pulse widths are shorter than 1 ms (the observational upper limit) then $L_{FRB}$ is correspondingly greater and the upper bound on the age of the most luminous

FRB correspondingly less.

The existence of such high field millisecond pulsars would not violate any law of physics, and Ostriker & Gunn (1971) suggested that they make supernovae. But they have never been observed, may lead to a conflict between SN and FRB rates (supernova remnant energies and the absence of pulsars in most SNR indicate they can only be an unusual subclass of neutron star births) and cannot explain the distribution of FRB dispersion measures (Katz 2016).

### B.2. Neutron star collapse

The collapses of *accreting* NS cannot be the explanation of FRB. Most neutron stars are observed to have masses of about 1.4 $M_\odot$, but the maximum mass of neutron stars must be at least 2.0 $M_\odot$ because a few such massive neutron stars are known. For accretion to push a 1.4 $M_\odot$ neutron star to collapse would require the release of at least $\sim 0.6\, M_\odot(GM/r) \approx 10^{53}$ ergs; and one such event per 1000 years in a galaxy implies a mean X-ray emission of about $3 \times 10^{42}$ ergs/s. This is about $10^3$ times the 2–10 keV X-ray luminosity of our Galaxy (Grimm, Gilfanov & Sunyaev 2002). Only if these hypothetical progenitors of FRB are born very close (within $\sim 10^{-3} M_\odot$) to their stability limit can the FRB rate be reconciled with the observed bounds on galactic X-ray emission. This argument would not exclude the collapse of rotationally stabilized (not accreting) NS as the result of angular momentum loss (Falcke & Rezzolla 2014) if they, like recycled pulsars, are inefficient ($\mathcal{O}(10^{-3}$–$10^{-4})$ Bogdanov, *et al.* (2006)) X-ray emitters. However, their mechanism of emission of a FRB remains obscure; the time scale of collapse (and disappearance of the NS magnetic moment) would be $10^{-4}$–$10^{-5}$ s, corresponding to emission at tens of kHz, not the observed frequencies $\sim 1$ GHz.

The recent discovery (Spitler, *et al.* 2016) of a repeating FRB excludes all models based on a catastrophic event that destroys the progenitor.

## C. SGR 1806-20

Tendulkar, Kaspi & Patel (2016) found that the Parkes telescope was observing a pulsar at the time of the giant 27 December, 2004 outburst of SGR 1806-20, and that the SGR was 31.5° above the horizon and 35.6° away from the beam direction. Analysis of the data found no evidence of a fast radio burst, with an upper limit tens of dB lower than predicted for a Galactic FRB out of beam (Katz 2014, 2016). This appears to contradict the suggestion that FRB and SGR outbursts are associated, but possible explanations should be considered:

**Atmospheric absorption:** SGR 1806-20 deposited about 1 erg/cm$^2$ of soft (30–100 keV) gamma-rays into the Earth's atmosphere at a depth of roughly 5 g/cm$^2$, where the molecular density is about $2 \times 10^{17}$ cm$^{-3}$. Approximately $2 \times 10^{10}$ electrons are produced per erg of deposited

energy, mostly distributed over a single scale height, and their recombination or capture time is long. Because of the high density, their collision rate (with neutral molecules) is high, absorbing energy from a propagating radio-frequency pulse. A rough calculation indicates an optical depth of about 0.02 for 1.4 GHz radiation, which is insignificant.

**Absorption at source:** SGR 1806-20 emitted at least $10^{46}$ ergs of soft gamma-rays, or about $2 \times 10^{53}$ photons. Some of these may be absorbed in a dense surrounding cloud, and if the cloud density exceeds $10^5/\mathrm{cm}^3$ the $\sim 30$ keV photoelectrons will each produce an additional $\sim 1000$ electrons by collision in the $\sim 1\,\mathrm{s}$ SGR duration. Such a cloud, with DM $\gtrsim 300$ $\mathrm{pc/cm}^3$, could be an effective absorber of $\sim 1$ GHz radiation, but only if it were close enough to the SGR (within $\sim 3 \times 10^{15}$ cm) to be fully ionized. Such a dense cloud that close to a neutron star, within a SNR, is implausible. In addition, only a fraction $\lesssim 10^{-2}$ of the energy of the $\sim 100\,\mathrm{ms}$ SGR flare is emitted in its $\lesssim 1\,\mathrm{s}$ rising edge assumed to correspond to the brief FRB.

**Propagation Broadening:** Tendulkar, Kaspi & Patel (2016) consider scattering (multipath) pulse broadening time scales in the range 14–56 ms, a range suggested by pulsar-derived models of interstellar propagation. However, Krishnakumar, *et al.* (2015) found that the most highly dispersed pulsars have broadenings of about $6 \times 10^4$ ms at 327 MHz, scaling ($\propto \nu^{-4.4}$) to about 100 ms at the frequency of observation of Tendulkar, Kaspi & Patel (2016). Pulsar searches are strongly biased against detection of highly broadened pulses and may be blind to highly dispersed objects, so gamma-ray selected objects in the Galactic plane (such as SGR) may be much more broadened than those discovered in pulsar surveys. Perhaps a radio burst from SGR 1806-20 was so broadened as not to have been detectable after filtering for pulsar-like rapid time variability.

**Rejection as interference:** A strong source far out of beam produces signals of similar amplitude in each of Parke's 13 beams. This is also a characteristic of interference (from local sources, or entering amplifiers by their "back doors"), and such signals may have been rejected as likely interference.

The rate of Galactic SGR is $\sim 0.1$/y, while the rate of observed FRB *per galaxy*, assuming cosmological distances, is $\sim 10^{-5}$/y per galaxy. Only a small subset of SGR can produce the observed FRB, and these may differ qualitatively from SGR 1806-20.

Tendulkar, Kaspi & Patel (2016) also compare the FRB rate to that of short GRB, a fraction $f < 0.15$ of which have been suggested (Nakar, *et al.* 2006; Ofek 2007) to actually have been SGR. Because of the comparatively low sensitivity of gamma-ray detectors, if these short GRB are associated with giant SGR outbursts at a ratio of 1:1 then comparison of the event rates indicates that they are detected only to a distance cutoff (assuming homogeneous distributions in Euclidean geometry) $0.013(f/0.15)^{1/3}$ of the FRB distance cutoff. If the latter is at $z = 1$ then the cutoff on SGR detection is about $55(f/0.15)^{1/3}$ Mpc, and a nominal gamma-ray fluence sensitivity of

$10^{-8}$ erg/cm$^2$ would correspond to an (isotropic) SGR energy of $4 \times 10^{45}(f/0.15)^{2/3}$ ergs. This is consistent with measurements of Galactic SGR, but uncertainty in $f$ and in the effective detector sensitivity make this a crude comparison.

## REFERENCES


Akgün, T., Miralles. J. A., Pons, A. & Cerdá-Durán, P. 2016 arXiv:1605.02253.

Bak, P., Tang, C., & Wiesenfeld, K. 1987 Phys. Rev. Lett. 59, 381.

Beloborodov, A. M. 2009 ApJ 703, 1044.

Beloborodov, A. M. & Li, X. 2016 arXiv:1605.09077.

Beloborodov, A. M. & Thompson, C. 2007 ApJ 657, 967.

Bjorken, J. D. & Drell, S. D. 1964 *Relativistic Quantum Mechanics* McGraw-Hill.

Bogdanov, S., Grindlay, J. E., Heinke, C. O., Camilo, F., Freire, P. C. C. & Becker, W. 2006 ApJ 646, 1104.

Burke-Spolaor, S., Bailes, M., Ekers, R., Marquart, J.-P., & Crawford, F. III 2011 ApJ 727, 18.

Champion, D. J., Petroff, E., Kramer, M., Keith, M. J., Bailes, M., Barr, E. D., Bates, S. D., Bhat, N. D. R., Burgay, M., Burke-Spolaor, S., Flynn, C. M. L., Jameson, A., Johnston, S., Ng, C., Levin, L., Possenti, A., Stappers, B. W., van Straten, W., Tiburzi, C. & Lyne, A. G. 2015 arXiv:1511.07746.

Chen, F. F. 1974 *Introduction to Plasma Physics* Plenum Press.

Cline, T. L. 1980 Comments Ap. 9, 13.

Cline, T. L., Desai, U. D., Pizzichini, G., Teegarden, B. J., Evans, W. D., Klebesadel, R. W., Laros, J. G., Hurley, K., Niel, M., Vedrenne, G., Estoolin, I. V., Kouvnetsov, A. V., Zenchenko, V. M., Hovestadt, D. & Gloeckler, G. 1980 ApJ 237, L1.

Connor, L., Sievers, J. & Pen, U.-L. 2015 MNRAS in press (arXiv:1505.05535).

Cordes, J. M. & Wasserman, I. 2016 MNRAS 457, 232.

Davis, L. 1947 Phys. Rev. 72, 632.

Falcke, H. & Rezzolla, L. 2014 A&A 562, 137.

Fishman, G. J., Meegan, C. A., Wilson, R. B., Brock, M. N., Horack, J. M., Kouveliotou, C., Howard, S., Paciesas, W. S., Briggs, M. S., Pendleton, G. N., Koshut, T. M., Mallozzi, R. S., Stollberg, M. & Lestrade, J. P. 1994 ApJS 92, 229.

Ganjadhara, R. T. 2010 ApJ 710, 29.

Ghosh, P. 2007 *Rotation and Accretion Powered Pulsars* World Scientific Publishing.

Gil, J. A. & Snakowski, J. K. 1990 å 234, 237.

Ginzburg, V. L. & Zhelezniakov, V. V. 1958 Sov. Astron. 2, 653.

Gold, T. 1968 Nature 218, 731.

Goldreich, P. & Julian, W. H. 1969 ApJ 157, 869.

Goodman, J. 1986 ApJ 308, L47.

Gould, R. J. 1972 Physica 60, 145.

Grimm, H.-J., Gilfanov, M. & Sunyaev, R. 2002 A&A 391, 923.

Hankins, T. H. & Eilek, J. A. 2007 ApJ 670, 693.

Heisenberg, W. & Euler, H. 1936 Z. Physik 98, 714.

Hones, E. W. & Bergeson, J. E. 1965 J. Geophys. Res. 70, 4951.

Hurley, K., Cline, T., Mazets, E., Barthelmy, S., Butterworth, P., Marshall, F., Plamer, D., Aptekar, R., Golenetskii, S., Il'inskii, V., Freeriks, D., McTiernan, J., Gold, R. & Trombka, J. 1999 Nature 397, 41.

Hurley, K., Boggs, S. E., Smith, D. M., Duncan, R. C., Lin, R., Zoglauer, A., Krucker, S., Hurford, G., Hudson, H., wigger, C., Hajdas, W., Thompson, C., Mitrofanov, I., Sanin, A., Boynton, W., Fellows, C., von Kienlin, A., Lichit, G., Rau, A., & Cline, T. 2005 Nature 434, 1098.

Jackson, J. D. 1962 *Classical Electrodynamics* Wiley, New York.

Katz, J. I. 1982 ApJ 260, 371.

Katz, J. I. 1986 J. Geophys. Res. 91, 10412.

Katz, J. I. 1996 ApJ 463, 305.

Katz, J. I. 2014 Phys. Rev. D 89, 103009.

Katz, J. I. 2016 ApJ 818, 19.

Krishnakumar, M. A., Mitra, D., Naidu, A., Joshi, B. C. & Manoharan, P. K. 2015 arXiv:1501.05401.

Kulkarni, S. R., Ofek, E. O., Neill, J. D., Zhang, A. & Juric, M. 2014 ApJ 797, 70.

Kulkarni, S. R., Ofek, E. O. & Neill, J. D. 2015 arXiv:1511.09137.

Kumar, D. & Ganjadhara, R. T. 2012 ApJ 746, 157.

Laros, J. G., Fenimore, E. E., Klebesadel, R. W., Atteia, J.-L., Boer, M., Kurley, K., Niel, M., Vedrenne, G., Kane, S. R., Kouveliotou, C., Cline, T. L., Dennis, B. R., Desai, U. D., Orwig, L. E., Kuznetsov, A. V., Sunyaev, R. A. & Terekhov, O. V. 1987 ApJ 320, L111.

Law, C. J., Bower, G. C. Burke-Spolaor, S., Butler, B., Lawrence, E., Joseph, T., Lazio, W., Mattmann, C. A., Rupen, M., Siemion, A. & VanderWiel, S. 2015 ApJ 807, 16.

Lorimer, D. R., Bailes, M., McLaughlin, M. A., Narkevic, D. J. & Crawford, F. 2007 Science 318, 777.

Lyubarsky, Y. 2014 MNRAS 442, L9.

Lyutikov, M. 2006 MNRAS 367, 1594.

Lyutikov, M. 2013 arXiv:1306.2264.

Manchester, R. N., Hobbs, G. B., Teoh, A. & Hobbs, M. 2005 AJ 129, 1993 `www.atnf.csiro.au/people/pulsar/psrcat/proc_form.pho?version=1` accessed Feb. 29, 2016.

Masui, K., Lin, H.-H., Sievers, J., Anderson, C. J., Chang, T.-C., Chen, X., Ganguly, A., Jarvis, M., Kuo, C.-Y., Li, Y.-C., Liao, Y.-W., McLaughlin, M., Pen, U.-L., Peterson, J. B., Roman, A., Timbie, P. T., Voytek, T., & Yadav, J. K. 2015 Nature 528, 523.

Mazets, E. P., Golenetskii, S. V. & Gur'yan, Yu. A. 1979 Sov. Astr. Lett. 5, 343.

McLaughlin, M. A., Stairs, I. H., Kaspi, V. M., Lorimer, D. R., Kramer, M., Lyne, A. G., Manchester, R. N., Camilo, F., Hobbs, G., Possenti, A., D'Amico, N. & Faulkner, A. J. 2003 ApJ 591, L135.

Melrose, D. B. & Yuen, R. 2016 arXiv:1604.03623

Nakar, E., Gal-Yam, A., Piran, T. & Fox, D. B. 2006 ApJ 640, 849.

Ofek, E. O. 2007 ApJ 659, 339.

Ostriker, J. P. & Gunn, J. E. 1971 ApJ 164, L95.

Palmer, D. M., Barthelmy, S., Gehrels, N., Kippen, R. M., Cayton, T., Kouveliotou, C., Eichler, D., Wijers, R. A. M., Woods, P. M., Granot, J., Lyubarsky, Y. E., Ramirez-Ruiz, E., Barbier, L., Chester, M., Cummings, J., Fenimore, E. E., Finger, M. H., Gaensler, B. M., Hullinger, D., Krimm, H., Markwardt, C. B., Nousel, J. A., Parsons, A., Patel, S., Sakamoto, T., Sato, G., Suzuki, M. & Tueller, J. 2005 Nature 434, 1107.

Parker, E. N. 1979 *Cosmical Magnetic Fields: Their Origin and Their Activity* Oxford U. Press.

Pen, U.-L. & Connor, L. 2015 ApJ 807, 179.

Petroff, E., *et al.* 2015 MNRAS 447, 246.

Popov, S. B. & Postnov, K. A. 2007 arXiv:0710.2006.

Popov, S. B. & Postnov, K. A. 2013 arXiv:1307.4924.

Priest, E. & Forbes, T. 2000 *Magnetic Reconnection* Cambridge U. Press.

Qin, Y., Liang, E.-W., Liang, Y.-F., Yi, S.-X., Lin, L., Zhang, B.-B., Zhang, J., Lü, H.-J., Lu, R.-J., Lü, L.-Z. & Zhang, B. 2013 ApJ 763, 15.

Ravi, V., Shannon, R. M. & Jameson, A. 2015 ApJ 799, L5.

Reid, H. A. S. & Ratcliffe, H. 2014 Res. Astron. Ap. 14, 773 arXiv:1404.6177.

Schwinger, J. 1951 Phys. Rev. 82, 664.

Soglasnov, V. A., Popov, M. V., Bartel, N., Cannon, W., Novikov, A. Y., Kondratiev, V. I. & Altunin, V. I. 2004 ApJ 616, 439.

Spitler, L. G., Scholz, P., Hessels, W. T., Bogdanov, S., Brazier, A., Camilo, F., Chatterjee, S., Cordes, J. M., Crawford, F., Deneva, J., Ferdman, R. D., Freire, P. C. C., Kaspi, V. M., Lazarus, P., Lynch, R., Madsen, E. C., McLaughlin, M. A., Patel, C., Ransom, S. M., Seymour, A., Stairs, I. H., Stappers, B. W., van Leeuwen, J. & Zhu, W. W. 2016 arXiv:1603.00581.

Stebbins, A. & Yoo, H. 2015 arXiv:1505:06400.

Tendulkar, S. P., Kaspi, V. M. & Patel, C. 2016 arXiv:1602.02188.

Thompson, C. & Duncan, R. C. 1992 ApJ 392, L9.

Thompson, C. & Duncan, R. C. 1995 MNRAS 275, 255.

Thompson, C., Lyutikov, M. & Kulkarni, S. R. 2002 ApJ 574, 332.

Thornton, D. 2013 Ph.D. thesis, University of Manchester, U. K.

Thornton, D., Stappers, B., Bailes, M., Barsdell, B., Bates, S., Bhat, N. D. R., Burgay, M., Burke-Spolaor, D. J., Champion, D. J., Coster, P., D'Amico, N., Jameson, A., Johnston, S., Keith, M., Kramer, M., Levin, L., Milia, C. Ng, Possenti, A. & van Straten, W. 2013 Science 341, 53.

Wang, P. F., Wang, C. & Han, J. L. 2014 MNRAS 441, 1943.

Widrow, L. M. 2002 Rev. Mod. Phys. 74, 775.

This preprint was prepared with the AAS LaTeX macros v5.2.